

# Exploring the Influence of Summer Temperature on Human Mobility during the COVID-19 Pandemic in the San Francisco Bay Area

Amina Ly<sup>1</sup>, Frances V. Davenport<sup>2</sup>, and Noah S. Diffenbaugh<sup>1</sup>

<sup>1</sup>Stanford University

<sup>2</sup>Colorado State University

December 20, 2022

## Abstract

Heat related illnesses are one of the leading causes of weather-related mortality in the United States, and heat extremes continue to increase in frequency and duration. Public health interventions include population mobility, including travel to central cooling centers or wellness checks on vulnerable populations. Using anonymized cellphone data from Safegraph's neighborhood patterns dataset and gridded temperature data from gridMET, we explored the mobility-temperature relationship in the San Francisco Bay Area at fine spatial and temporal scale. We leveraged spatial variability in median income and temporal variability in COVID-19 related policies across two summers (2020-2021) to analyze their influence on the mobility-temperature relationship. We completed quantile regressions for a dataset stratified by income and year. We found that mobility increased at a higher rate with higher temperatures in 2020 than 2021. However, in 2021, the relationship reversed for several wealthier income groups, where mobility decreased with higher temperatures. We then augmented the analysis and calculated a panel regression with fixed effects to characterize the mobility-temperature relationship while controlling for temporal and spatial variability. This analysis suggested that all areas exhibited lower mobility with higher summer temperatures. However, similar to the results of the quantile regression, the rate of decrease in mobility in response to high temperature was significantly greater among the wealthiest census block groups compared with the least wealthy. Given the fundamental difference in the mobility response to temperature across income groups, our results are relevant for heat mitigation efforts in highly populated regions in current and future climate conditions.

## Hosted file

952253\_0\_art\_file\_10543698\_rn0291.docx available at <https://authorea.com/users/567902/articles/613998-exploring-the-influence-of-summer-temperature-on-human-mobility-during-the-covid-19-pandemic-in-the-san-francisco-bay-area>

## Hosted file

952253\_0\_supp\_10543766\_rn042x.docx available at <https://authorea.com/users/567902/articles/613998-exploring-the-influence-of-summer-temperature-on-human-mobility-during-the-covid-19-pandemic-in-the-san-francisco-bay-area>

# Exploring the Influence of Summer Temperature on Human Mobility during the COVID-19 Pandemic in the San Francisco Bay Area

Amina Ly<sup>1\*</sup>, Frances V. Davenport<sup>1,2,3</sup> and Noah S. Diffenbaugh<sup>1,4</sup>

<sup>1</sup> Department of Earth System Science, Stanford University, Stanford, CA, USA

<sup>2</sup> Department of Atmospheric Science, Colorado State University, Fort Collins, CO, USA

<sup>3</sup> Department of Civil and Environmental Engineering, Colorado State University, Fort Collins, CO, USA

<sup>4</sup> Doerr School of Sustainability, Stanford University, Stanford, CA, USA

Corresponding author: Amina Ly ([aminaly@stanford.edu](mailto:aminaly@stanford.edu))

## Key Points:

- We investigate the influence of summer temperatures on a normalized mobility indicator in the San Francisco Bay Area for summer 2020-2021.
- Mobility response to temperature was sensitive to regional public health policies and local factors such as median income of destinations.
- Wealthier areas generally had lower mobility during periods of severe heat, compared with other income groups.

## Abstract

Heat related illnesses are one of the leading causes of weather-related mortality in the United States, and heat extremes continue to increase in frequency and duration. Public health interventions include population mobility, including travel to central cooling centers or wellness checks on vulnerable populations. Using anonymized cellphone data from Safegraph's neighborhood patterns dataset and gridded temperature data from gridMET, we explored the mobility-temperature relationship in the San Francisco Bay Area at fine spatial and temporal scale. We leveraged spatial variability in median income and temporal variability in COVID-19 related policies across two summers (2020-2021) to analyze their influence on the mobility-temperature relationship. We completed quantile regressions for a dataset stratified by income and year. We found that mobility increased at a higher rate with higher temperatures in 2020 than 2021. However, in 2021, the relationship reversed for several wealthier income groups, where mobility decreased with higher temperatures. We then augmented the analysis and calculated a panel regression with fixed effects to characterize the mobility-temperature relationship while controlling for temporal and spatial variability. This analysis suggested that all areas exhibited lower mobility with higher summer temperatures. However, similar to the results of the quantile regression, the rate of decrease in mobility in response to high temperature was significantly greater among the wealthiest census block groups compared with the least wealthy. Given the fundamental difference in the mobility response to temperature across income groups, our results are relevant for heat mitigation efforts in highly populated regions in current and future climate conditions.

## Plain Language Summary

The health risks associated with extreme heat are increasing with climate change. There are a number of steps taken by public health officials that rely on local travel, including public cooling shelters and wellness checks. We used anonymized cellphone data and gridded daily temperature data to explore how mobility responded to temperature variations in the San Francisco Bay Area during the summer months of 2020 and 2021. Our analysis found that when our dataset was separated by income and year, mobility increased with higher temperatures for nearly all subgroups in 2020. In 2021, some wealthier areas exhibited the reverse relationship, with mobility decreasing at higher temperatures. When we completed another analysis that controlled for variability in time and space, all areas exhibited decreased mobility with higher summer temperatures, but the wealthiest areas decreased faster than the least wealthy areas. These differences among income groups make our results particularly relevant for heat management practices in highly populated regions, both now and in the future.

## 1 Introduction

Exposure to extremely hot conditions is detrimental to many aspects of human health and wellbeing (Duffy et al., 2019). Excessively high temperatures that lead to heat-related illnesses remain one of the leading causes of mortality in the United States (US) due to extreme weather (CDC, 2019). Hot extremes increase hospitalizations, emergency room visits, use of emergency transport (Onozuka & Hagihara, 2015, Liss & Naumova, 2019), incidences of cardiovascular

mortality (Wainwright et al., 1999), suicide (Burke et al., 2018), violence (Hsiang et al., 2013, Burke et al., 2018), risk of premature mortality (Schwartz et al., 2015), low birth weights (Deschênes et al., 2009), and kidney stones (Tasian et al., 2014). Heat can also have an adverse effect on necessary daily activities and lead to increased workplace injuries (Park et al., 2021), sleep loss (Obradovich et al., 2017, Zheng et al., 2019) and reduced appetites (Zheng et al., 2019). In the US, incidents of extreme heat have increased in both intensity and duration since the 1960s (USGCRP, 2018, IPCC, 2021). This trend is anticipated to continue into the rest of the century even in aggressive decarbonization scenarios (Collins et al., 2013, Diffenbaugh & Ashfaq, 2010, Diffenbaugh et al., 2018), thereby increasing the exposure of the US population to these events (Reidmiller et al. 2018, IPCC, 2021, Batibeniz et al. 2020).

Mobility is one way that individuals and populations respond and adjust to extreme temperatures—in general, as temperatures rise on an annual cycle, so does mobility (Böcker et al., 2016, Liu et al., 2014). Typically, heat stress is managed using air conditioning, public cooling centers, and public awareness campaigns and warning systems (Bassil et al., 2009, Eisenman et al., 2016, Palecki et al., 2001). Many of the interventions that combat the risks of intensifying heat events include some amount of local travel. This includes traveling to cooling centers and conducting wellness checks on vulnerable individuals who lack air conditioning (Widerynski et al., 2017). Characterizing typical mobility patterns in response to increasing temperatures is thus critical for minimizing health risks associated with extreme heat exposure by anticipating the potential need for wellness services during heatwaves, supporting accessibility efforts, and limiting strain on public health services.

The COVID-19 pandemic provides a unique context in which to explore the influence of social and policy pressures on mobility patterns during periods of extreme heat. After the declaration of a worldwide pandemic by the World Health Organization in March 2020 (WHO 2020), numerous countries began to implement travel and mobility restrictions as their main non-pharmaceutical intervention to reduce the number of COVID-19 infections within their borders. By April 20th 2020, 100% of travel destinations had some form of travel restrictions in place, of which 45% partially or completely closed borders to tourists, 18% banned individuals traveling from select countries, and 7% applied quarantine or self-isolation requirements (UNWTO 2020).

In the US, individual states and counties implemented their own restrictions, with regulations often differing between neighboring municipalities. Twenty-four states established travel restrictions that included periods of isolation and testing requirements for those entering the state (Studdert et al., 2020). Government responses have been highly variable in space and time as individual states and municipalities instituted their own guidelines and ordinances in the absence of blanket federal orders (Diffenbaugh et al., 2020). COVID-19 Shelter in Place (SIP) protocols did change mobility patterns across the country, and many regions saw an increase in the frequency of visitations to public, outdoor spaces (Wu et al., 2021). California specifically implemented travel guidance and allowed counties to impose additional restrictions as they saw fit (Aragón, 2020). Workplace and school closures were calculated to be effective measures in avoiding COVID-19 deaths in the San Francisco (SF) Bay Area (Head et al., 2020). As a result of CDC and state guidance, and quantitative models supporting the efficacy of closures, schools and ‘non-essential’ businesses were closed and shifted to a virtual environment.

The SF Bay Area was one of the early epicenters of COVID-19 transmission in the US, and since then has consistently seen some of the country's most restrictive pandemic management policies (Studdert et al., 2020). Beginning with a multi-county stay-at-home order in March 2020, these SIP policies heavily restricted business operations and travel for the subsequent year. In addition, the SF Bay Area has the second lowest rates of at-home cooling among major metropolitan areas in the US, with only 47% of households reporting at-home air conditioning in 2019 (American Housing Survey, 2018, Jung, 2021). This means that a majority of households rely on cooling methods other than domestic air-conditioning during periods of extreme heat. Further, the region exhibits a classic summer-dry "Mediterranean" climate (Hobbs et al., 1995, Ekstrom & Moser, 2012), enabling investigation of the influence of temperature on mobility in the absence of the potentially confounding effect of precipitation variability during the hot season. For these reasons, the SF Bay Area region is an ideal testbed to further investigate the relationship between temperature and mobility in the context of the pandemic.

Several studies have identified that differences in socio-economic status (O'Neill et al., 2005, Vant-Hull et al., 2018) and the built environment (Eisenman et al., 2016, Gronlund & Berrocal., 2020) are associated with varied vulnerability to extreme heat exposure throughout the US. This heterogeneity in socio-demographics points to the value of considering how these spatially defined characteristics may result in varied responses to both policy decisions and climatic conditions. In addition, given the role mobility plays in public health interventions for heat illness, and the persistent influence of socio-demographic differences on public health outcomes, it is important to consider the response to severe heat in the context of policy decisions intended to minimize the spread of COVID-19. To that end, we used data from personal mobile devices to characterize the small-scale, daily movement patterns across the SF Bay area throughout the pandemic period of 2020-2021. We then used both quantile regression and panel regression with fixed effects to characterize the relationship between income and mobility during the summer months.

## 2 Materials and Methods

### 2.1 Data

We utilized the gridMET 4-km gridded daily maximum temperature data (Abatzoglou, 2013) to calculate temperature in the SF Bay Area region. To quantify the impact of high temperatures on mobility, we selected all data from May to September, when hot temperatures are most likely to occur in the region. Using the 2020 census block group boundaries from the US Census, we calculated the mean daily high temperature of all grid cells within each CBG to obtain a time series of the high temperature by CBG each day from 1979-2021. We used the 2019 US Census Bureau's American Community Survey's (ACS) 5-year Estimates of population and median income by CBG (US Census Bureau, 2022)

We analyzed mobility patterns using the SafeGraph Neighborhood Patterns dataset (SafeGraph 2022). This dataset was created by analyzing anonymized pings from mobile devices, and contains footfall data for each CBG from January 2018 to the present day. For this analysis, we only utilized data starting in 2020. Any devices that were recorded in a CBG for a duration of

less than a minute were removed, and the remaining devices were counted as a “stop”. Each stop datapoint included information on the date, hour, and CBG of the recorded stop. Due to data constraints associated with Safegraph’s privacy policy, the source information included only the number of devices that spent time in the CBG and did not contain information about whether a stop was made by a home device or a non-resident device. An accompanying Safegraph dataset contained a monthly estimate of the total number of home devices based on devices’ nighttime activity. Safegraph added laplacian noise as a differential privacy technique to protect individual privacy.

Wildfires in the Bay Area in the summer and autumn of 2020 and 2021 caused several poor air quality days where residents were instructed to limit travel and remain indoors (Bay Area Air Quality Management District’s (BAAQMD), 2022). In order to exclude the influence of days where this additional public intervention was introduced, we removed data points from all datasets for the 12 days on which at least one county in the SF Bay Area recorded a BAAQMD Air Quality Index value of  $\geq 151$  (for which the BAAQMD recommends all individuals should limit prolonged outdoor exertion).

## 2.2 Creation and interpretation of mobility index

Using the Safegraph dataset, we created a mobility index (MI) that allowed us to compare mobility across CBGs, and thereby characterize movement across the SF Bay Area. We estimated the daily number of visits as the number of total stops minus home devices in that CBG. We then normalized the difference using the number of home devices for each block group to calculate our final MI value. We calculated MI daily for each census block group from January 2020 through December 2021.

This MI index was designed to address some of the limitations of the Safegraph dataset, such as the ambiguity between stops by visitors and stops by home devices. These limitations should be considered when interpreting the MI values. By subtracting out the devices identified by Safegraph as “home devices” we assumed that the remaining number of devices are either “visitors” to the location or a home device that left and returned that day. Due to these constraints, MI should be interpreted as a normalized indicator of the amount of travel into a CBG on a given day—including any home device that left and returned on that day.

## 2.3 Census block group analysis

To further understand how demographics may influence the relationship between a CBG and mobility during the hottest part of the year, we used ACS’s 5-year estimates of population and median income by CBG. We assigned each CBG to an income group between 1 (“Low” income) and 5 (“High” income). We weighted this grouping by population, so that the Low income group represented the lowest earning 20% of the population in the SF Bay Area, the Medium Low income group the lowest 20%-40% of earners, and so on. This weighting ensured that there were roughly the same number of individuals represented in each income group.

We plotted the distribution of the MI for each income group. In addition, we tested whether the distributions were different between income groups by comparing all pairings of income groups

using two non-parametric tests: a two-sample Kolmogorov-Smirnov (K-S) test, and a Wilcoxon Rank Sum Test. The K-S test is sensitive to differences in both location and shape of the distributions, and the null hypothesis is that the two samples are drawn from the same underlying distribution. The Wilcoxon test's null hypothesis is that the two distributions are the same and have the same median.

## 2.4 Quantile regression

We used quantile regression to analyze the effect of temperature changes across the distribution of MI values during the summer months (May - September):

$$[1] Y_{\theta g} = \beta_{\theta} X_g + \varepsilon_{\theta g}$$

where  $Y$  is the expected daily mobility index (MI) value for income group  $g$  in percentile  $\theta$ ;  $\beta$  is the estimated coefficient of percentile  $\theta$ ;  $X$  is the average daily maximum high temperature of a CBG in income group  $g$ .  $\varepsilon_{\theta g}$  is an unspecified error term, consistent with other nonparametric quantile regression models.

The quantiles  $\theta$  included in this analysis were the 25th, 50th, 75th, and 95th of calculated MI values. These quantiles represented the least-mobile to most-mobile CBGs, based on daily MI values. Some CBGs were categorized in the same quantile almost every day (e.g., a residential area), some were higher during certain parts of the week (e.g., commercial use office spaces), and others were occasionally categorized in the higher quantiles (e.g., a CBG housing a stadium).

We stratified the dataset by our assigned income groups to explore how the response across the MI distribution may be influenced by the underlying income characteristics of each CBG. Calculated MI values across the SF Bay Area were heavily skewed and contained a number of outliers and extreme values (Figure S1). We used quantile regression to limit the amount of distortion from these values (Buchinsky, 1998), and to analyze the response of a specific subset of the response variable. We also stratified our data by year to explore the difference in our response variable during a period of strict SIP policies (2020) and the subsequent summer after most restrictions were lifted (2021).

## 2.5 Panel Regression with Fixed Effects

We complemented our quantile regression analysis with a linear panel regression with fixed effects, which is a causal inference technique that enabled us to establish a deeper understanding of how sensitive mobility is to the daily high temperature of a given CBG. Our main specification tested a cube root relationship between MI and temperature:

$$[2] \sqrt[3]{Y_{ct}} = \beta X_{ct} + n_c + \delta_t + \varepsilon_{ct}$$

where  $Y_{ct}$  is the expected mobility index (MI) value in CBG  $c$  on a given day  $t$ ;  $\beta$  is the estimated coefficient;  $X$  is the average daily maximum high temperature of CBG  $c$  on day  $t$ ;  $n_c$  is the CBG fixed effect;  $\delta_t$  is the year, month, and week-of-year fixed effect created by concatenating the

year, month, and number of complete seven day periods that have occurred between the date and January 1st of the year; and  $\varepsilon_{ct}$  is an error term.

This method was particularly valuable because it controlled for invariant differences between CBGs, subtracted out average differences in mobility between them, and accounted for any differences in SIP orders between the different sub-regions of the SF Bay Area. The time fixed effects variable subtracts out month-to-month, week-of-year, and annual mobility variations—accounting for seasonal changes, as well as shifts in mobility due to week-to-week variation driven by holidays and short-term shocks, and annual differences between 2020 and 2021. When compared to using a daily time fixed effects variable, the week, month, and year fixed effect led to a smaller 95% confidence interval (Figure S2). With these controls, this model isolated the effect of temperature on mobility from spatial and temporal confounding factors.

We used the daily high temperature within each CBG as the independent variable, and the calculated MI value for that day in each census block group as the dependent variable. We transformed the MI for this analysis by taking the cube root of MI values. To do so, we took the cube root of the absolute value of each MI, and multiplied the result by the sign of the original MI. Unlike a log transformation, this strategy allows us to maintain zeros and negative MI values while addressing the skewed MI values (Figure S1). In addition, we completed supplementary calculations with log-transformed MI values (where 1.0001 was added to each MI value), and compared those results to the cube root transformed dataset (Figure S2).

This first panel regression analysis pooled all income groups. We then performed a second analysis by adding in median income as an interaction term. We utilized median income as a proxy for a number of factors that may influence mobility and are correlated with income at the CBG level. These include socio-economic status, population density, infrastructure, and land use type. We characterized the relationship between temperature and mobility across five income groups, again using a cube root specification:

$$[3] \sqrt[3]{Y_{ct}} = \beta X_{ct} I_g + n_c + \delta_t + \varepsilon_{cit}$$

where  $Y_{ct}$  is the expected mobility index (MI) value in CBG  $c$  on a given day  $t$ ;  $\beta$  is the estimated coefficient;  $X$  is the average daily maximum high temperature of CBG  $c$  on day  $t$ ;  $I_g$  is the CBG's assigned population-weighted income group;  $n_c$  is the CBG fixed effect;  $\delta_t$  is the month, week of year, and year fixed effect;  $\varepsilon_{cit}$  is an error term.

For all panel regression models, we only used data from May to September. We estimated the 95% confidence intervals using a bootstrap resampling technique. We resampled the original data by county with replacement to obtain a new dataset of the same length as the original dataset, and re-ran the same regression on the new subset. We repeated this process 1000 times to obtain a range of model outputs. Of the resulting model coefficients, we used the 2.5 and 97.5th percentile coefficient values as the minimum and maximum values for our 95% confidence interval range.

### 3 Results



As expected, from May to September (which we refer to as ‘summer’) in 2020 and 2021, areas closer to the ocean tended to experience cooler temperatures ( $\sim 20^{\circ}\text{C}$ ), while those further inland experienced much higher average summer temperatures ( $\sim 30^{\circ}\text{C}$ ) (Figure 1, Panel A). Likewise, inland CBGs had more days with temperatures at or above  $34^{\circ}\text{C}$ , as opposed to CBGs closer to the coast or San Francisco Bay (Figure S3).

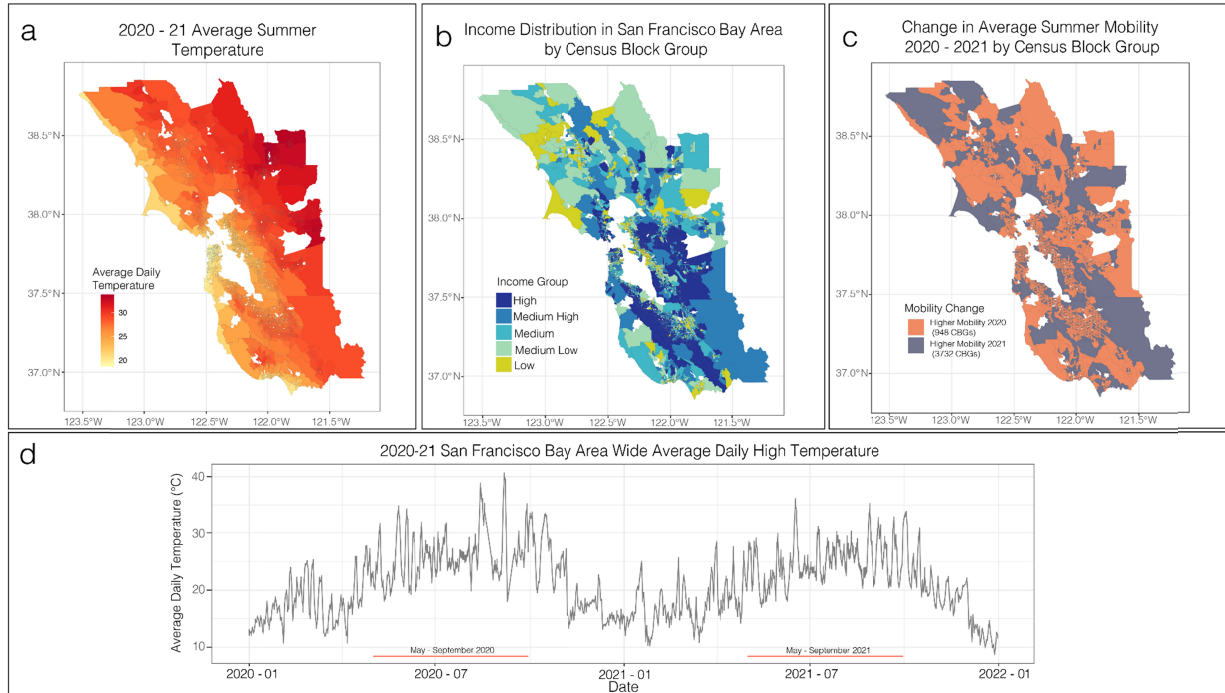


**Figure 1.** Overview of data included in analysis. (a) Daily high temperature was calculated by averaging the maximum daily temperature of all gridMET grid cells within a census block group (CBG) each day. (b) Each CBG was assigned an income group between 1 (Low income) and 5 (High income). Income groups were weighted by population (see Materials and Methods). (c) Mobility index change was calculated as the sign of the difference between 2020 and 2021. CBGs with a higher value in 2020 are shown in orange; CBGs with a higher value in 2021 are shown in purple. (d) Region-wide average daily temperature in 2020 and 2021 for the San Francisco Bay Area. Average summer temperature (a) and mobility (c) only reflect data for days between May and September, which are delineated in red along the x-axis in (d). Temperature recordings from October 28, 2021 - October 31, 2021 were removed from the gridMET dataset due to suspected record error. Analysis did not include data in this month, and therefore did not affect further reported results.

As reported by the ACS, the median annual income of CBGs in the SF Bay Area ranged from \$11,406 to \$250,001, with the average value across all CBGs in the SF Bay Area being  $\sim \$95,774$  (median = \$88,000) (Figure 1, Panel B). We grouped CBGs into different income groups by population to investigate the variable responses to MI by income. From lowest earning to highest, the Low income CBGs had a median income from \$11,406 to \$57,426; Medium Low income CBGs had a median income from \$57,446 up to \$76,985; Medium income CBGs had a median income from \$77,000 to \$99,792, Medium High income CBGs had a median income

from \$99,803 to \$129,375, and High income CBGs had a median income of \$129,421 to \$250,001. Each group represented 20% of the population of the SF Bay Area.

Our mobility index (MI) estimated the number of visits to a CBG, normalized by the number of residents. The largest decrease in MI took place from mid-March to early-April of 2020—coinciding with the SIP policies that began on March 16th, 2020, in SF Bay Area counties (San Francisco Department of Health (SFDoh), 2020). The mean MI during the first 30 days of SIP policies was 0.15, with the lowest recorded MI value of -0.47 on March 31<sup>st</sup>, 2020. By definition, a negative MI value indicates fewer devices entering the CBG – including returning home devices – than the number of recorded home devices, and the minimum possible value is -1.0. The average MI in all of 2020 and 2021 was 1.20 (median = 0.69), and 1.24 (median = 0.71) in the summer. In 2020, our calculated MI was generally lower on days when temperatures exceeded 34°C (mean = 0.86, median = 0.50) than in 2021 (mean = 1.60, median = 0.96) (Figure 1, Panel C). Of the 4722 CBGs included in the calculation, 3766 (80%) increased in mobility from 2020 to 2021. Of those 3766, 3026 (80.3%) experienced at least a 50% increase in mobility.

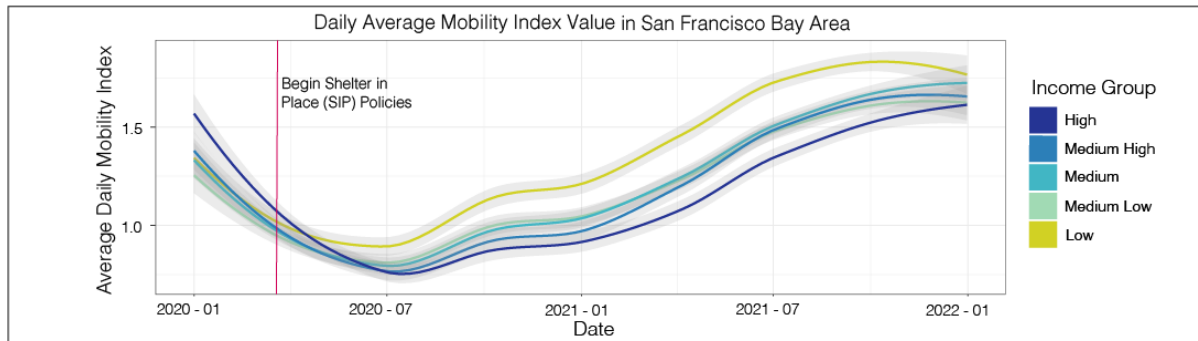


**Figure 2.** Loess regression of all calculated Mobility Index (MI) values from January 2020 through December 2021, by income group. The shaded area represents the 95% confidence interval of the loess regression. Shelter in Place policies began on March 16th, 2020.

In the first few months of 2020, prior to the start of SIP policies, the average MI values were similar among most income groups (Figure 2). The 95% confidence interval of the loess regression was indistinguishable for CBGs with a median household income below \$130,000/year (comprising the Low to Medium High income groups). In contrast, CBGs in the High income group (i.e., those with a median household income above ~\$130,000/year) had an average MI that was higher than the other groups in early 2020. However, there was a noticeable shift in relative MI by income group as the start of the COVID pandemic led to implementation of SIP policies and closures of many public spaces. CBGs in the Low income group (~<\$57,000/year) had the highest average MI by mid-2020, a pattern that continued through the end of 2021. Meanwhile, CBGs in the High income group consistently had the lowest average MI through the end of 2021 (Figure 2).

The mean MI value changed for many CBGs over the course of the two-year study period. The distribution of summer MI was different between the income groups (Figure 3,). For all pairings of income groups, we reject the null hypothesis of the K-S test. For most pairings, we reject the

null hypothesis of the Wilcoxon test; the only exceptions were in 2021 between the High income and Medium income groups, High and Low income groups, and Medium and Low income groups in 2021 (Figure 3, Panel B).

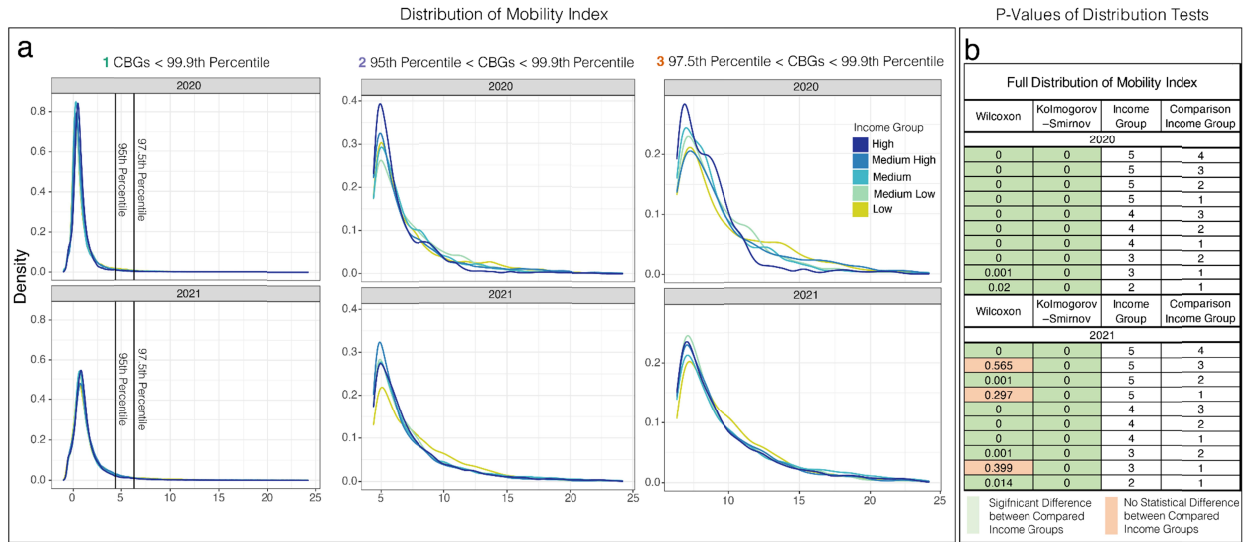


**Figure 3.** Distribution of calculated mobility index (MI) by income group. (a) Density distribution displayed included values up to the 99.9th percentile (MI = 24.2). (b) All pairings of income groups were compared using a two-sample Kolmogorov-Smirnov (K-S) test, and a Wilcoxon Rank Sum Test. Tests where the p-value was  $\leq 0.05$  were considered significant and highlighted in green; tests where the p-value was  $>0.05$  are highlighted in orange.

Given these differences between income groups and SIP policies in 2020 and 2021, we used quantile regression for each income group and year separately to quantify the change in temperature across the distribution of recorded MI values. Across all income groups, the CBGs with MI values in the 95th percentile were the most sensitive to a unit change in temperature in their respective year (Figure 4). The two models constructed for 2020 and 2021 both predicted that as temperatures increase, the most visited Low income CBGs would experience an increase in MI of  $\sim 0.1$  per  $^{\circ}\text{C}$  increase. Conversely, for the most visited High income CBGs, the two models predicted decreases in MI of  $\sim 0.005$  per  $^{\circ}\text{C}$  increase in 2020 and  $\sim 0.08$  per  $^{\circ}\text{C}$  increase in 2021. These results suggest an opposite response of mobility to increasing temperature between the most visited Low and High income CBGs. Further, in 2020, all coefficients were unambiguously positive except for one, which would indicate an increase in mobility with increasing temperature. (The single exception was in the 95th percentile of MI in the High income group, which had a negative coefficient and a confidence interval that crossed 0.) In 2021 this pattern did not hold, as several coefficients were negative (some of which were significant). Notably, the Low income group was the only group that did not have any negative coefficient values in either year.

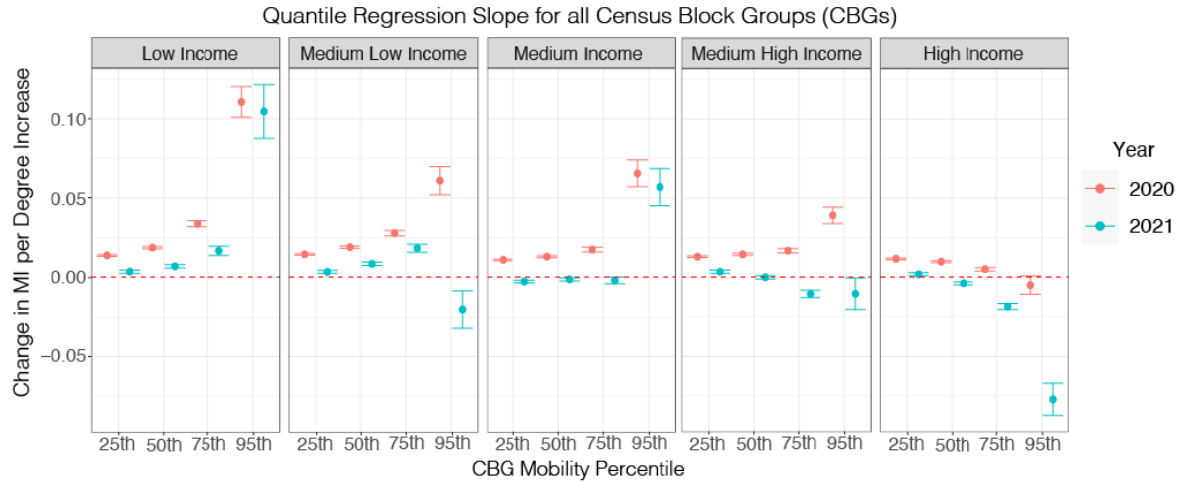


**Figure 4.** Effect of temperature on mobility index for each income group for 2020 and 2021. Effects were measured as the change in MI per °C increase. Points show median coefficient estimates and vertical bars show the 95% CI around each point estimate.

Given the relationship between MI and temperature revealed by the quantile regression, we extended our analysis using a linear panel regression with fixed effects (Figure 5, Panel A). The results are plotted as the change in MI as temperatures deviate from the median temperature in the SF Bay Area during this period (24°C). The calculated coefficient for the response of MI to variations in temperature was -0.0024, with a p-value <0.05. Hence, for every 10°C increase in temperature, the  $\sqrt[3]{\text{MI}}$  can be expected to decrease by about 0.024. To aid in interpretation, we repeated this analysis using a log-transform of MI rather than  $\sqrt[3]{\text{MI}}$ , which yielded a similar prediction of ~2% decrease in MI for every 10°C increase in temperature (Figure S2).

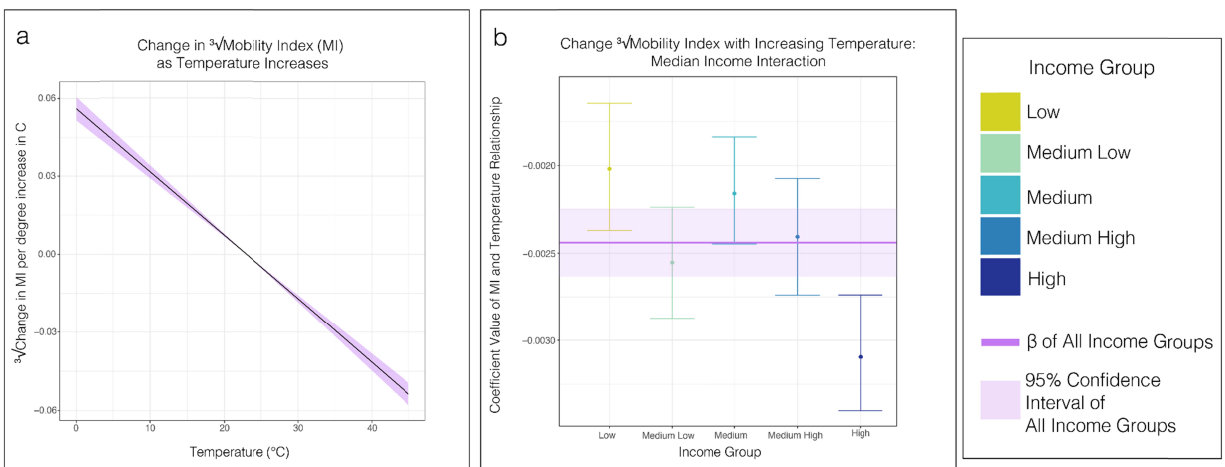


**Figure 5.** Effect of temperature on mobility index using fixed effects regression model. (a) Relationship between temperature and  $\sqrt[3]{\text{Mobility Index (MI)}}$  across the San Francisco Bay Area.

Median regression model shown with solid purple line. Purple shading indicates 95% CI estimated by bootstrapping by county with replacement (see Materials and Methods). Response function was centered at the mean summer temperature for 2020-2021 (24°C). (b) Resulting relationship between MI and temperature after the income group interaction variable is integrated into the model. Points show median coefficient estimates and vertical bars show the 95% CI around each point estimate. Solid purple line and shaded area are model results from (a) for comparison.

To explore how socio-economic differences may have influenced the relationship between mobility and temperature, we added a median-income interaction term to the panel regression model (Figure 5, Panel B). The coefficients for all income groups were negative (implying decreased mobility in response to higher temperatures), and each had a p-value of <0.001. The Low income group had the least negative coefficient (implying the least reduction in mobility in response to higher temperatures), while the High income group had the most negative coefficient (implying the greatest reduction in mobility in response to higher temperatures). Although there was substantial overlap in the confidence intervals for the three intermediate income groups (Medium Low, Medium and Medium High), the confidence intervals for the highest and lowest income groups were entirely distinct from each other. Further, the confidence interval for the highest income group (High) was distinct from even the confidence interval for the pooled fixed effect model that did not distinguish between income groups.

#### 4 Discussion

Much of the temperature and mobility research in the context of COVID-19 has centered on viral transmission. Although temperature is negatively related to COVID-19 transmission (Shao et al., 2021), higher temperatures are positively associated with mobility (Badr et al., 2020, Zhu et al., 2020). Shao et al. (2021) reported that mobility has a suppressing effect on the temperature-transmission relationship. Likewise, Wu et al. (2021) investigated how weather and mobility may have interacted during the first year of the COVID-19 pandemic by calculating the correlation between weather and mobility in different US states specifically during 2020, and found a weakly positive correlation between temperature and park visits on days without rain. These studies explored the dynamics of mobility and COVID-19 to bring additional insight to the public health implications of COVID-19 policies and the compounding effects of high temperatures.

We augmented this research on pandemic-era temperature-mobility relationships by incorporating the critical element of socio-demographic spatial heterogeneity in a highly populated region that contains both metropolitan and rural areas. Thus, our work has the potential to offer new insight into differences in the response of mobility to temperature across income groups. In addition, by extending the study period through the summer of 2021, our analysis included periods of the pandemic with additional COVID-19 virus variants (Vasireddy et al., 2021) and a wider range of SIP policies.

Our mobility metric captured the decline in mobility in the SF Bay Area following the establishment of SIP policies in spring of 2020 (Figure 2, Panel A). For the two years we analyzed, average mobility was higher in 2021, coinciding with relaxed SIP restrictions.

Throughout this two-year period, we found a link between our mobility metric and the median income of a CBG, with the highest earning CBGs associated with a more rapid decrease in MI value in response to increasing temperatures. This means either that wealthier residents of these neighborhoods traveled in and out of their CBG less frequently, and/or that fewer outside visitors entered the CBG.

In the context of the COVID-19 pandemic, these wealthy CBGs exhibited a pattern of lower mobility that aligned with the intended effects of SIP policies (i.e., reduction or cessation of non-essential travel, shifting to remote work when possible, and limits on gatherings in an attempt to reduce virus transmission). Conversely, lower income CBGs showed a pattern of movement that was less aligned with the intended effects of SIP policies (i.e., either increased travel (Figure 4) or limited reductions when compared to other subsets of the population (Figure 5)). Notably, any medically necessary travel was considered ‘essential’ and therefore travel completed to reduce exposure to extreme heat and protect personal health was allowable under SIP (SFDoH 2020, Newsom 2020); however, such travel required individuals to choose between continued heat exposure at home and the risk of exposure to COVID-19 outside the home. Since the median income value in our analysis was attributed to the visited CBG, we cannot draw conclusions about the income status of those visiting the CBGs.

While the COVID-19 pandemic was on-going throughout the study period, the SIP orders and unique social environment of the period were not uniform across the region. The strict closure of all non-essential businesses and travel restrictions in 2020 gave way to limited closures and capacity restrictions after the introduction of vaccines in early 2021. These unique conditions allowed us to examine the variation in response across the population, and further understand how public health policies interact with the communities they aim to protect within the context of extreme heat.

The effects of these changes were found in our regressions (Figure 4, 5). In 2020, nearly all CBGs had an MI that increased with increasing temperature in our quantile regression (Figure 4). In 2021, when most SIP orders were lifted, many CBGs exhibited decreasing MI values with increasing temperature. One major exception to this pattern was in 2020: CBGs in the 95th percentile of MI values in the High income group (>\$130,000/year) exhibited decreasing MI values with increasing temperature. The strictest SIP orders were in effect during the summer of 2020, yet the quantile regression showed that only the wealthiest CBGs displayed potential evidence of decreasing mobility with increasing temperature, while other places around the SF Bay Area exhibited increasing mobility. Likewise, in our fixed effect model with income interaction (Figure 5, Panel B), we found that although all income groups exhibited decreasing mobility with increasing temperature, the wealthiest CBGs displayed the largest decrease, and were statistically distinct even when compared to a model that included all income groups. One possible interpretation is that as temperatures increased, areas that were wealthy (and thus more likely to have access to air conditioning or other heat abatement at home) could continue to comply with SIP orders.

Further, while the results of the quantile regression suggested that the response of mobility to temperature was stronger and more positive (i.e., above 0) in 2020 than in 2021, nearly all Low and Medium Low income CBGs still exhibited increasing MI with increasing temperature in

2021 (Figure 4). Likewise, while the fixed effects model with income interaction (which pooled all MI quantiles, as well as the years 2020 and 2021) predicted a decrease in mobility in response to increasing temperature for all income groups, the Low income group had a significantly smaller rate of mobility reduction than the High income group (Figure 5). These results could potentially indicate, for lower income groups, either (i) reliance on mobility to alleviate the impacts of extreme heat, or (ii) fewer options to reduce mobility due to work or personal obligations.

The distribution of average MI values were right skewed and there were a number of CBGs with MI values that were an order of magnitude higher than the average (Figure S1). These locations represented areas that are highly trafficked, and often included points of interest (e.g., retail centers, tourist attractions, and downtown areas (Table S1)). We found that CBGs with MI values that fell into these extreme quantiles (95th percentile) often responded differently than the lower quantiles as temperature increased, and that the median income of the CBG can be important in determining the direction and/or magnitude of that response (Figure 4).

It is important to emphasize that income alone cannot fully explain all of the disparity in environmental (Banzhaf et al., 2019) and health (Zimmerman & Anderson, 2019) outcomes. The population of the SF Bay Area has variable sensitivities to extreme heat due to known risk factors such as prevalence of at-home cooling access (O'Neill et al., 2003), median age (Luber and McGeehin, 2008), racial background (Basu and Ostro, 2008), and ethnic background (Hansen et al., 2013). We stratified our data by income, which is known to itself influence health and wellbeing and is also correlated with other risk factors (Downey 1998, Reid et al., 2009). However, while our study offers additional insight into mobility responses to severe heat within a highly populated region with severe income inequality, it does not offer a fully exhaustive directory of CBGs most likely to see a change in MI on a hot day.

In addition to socioeconomic heterogeneity, the SF Bay Area also encompasses substantial climatic heterogeneity, including coastal and inland regions. The high variety of geographic features — including topography (mountains, inland valleys), and coastal exposure (Ekstrom & Moser, 2012) — contributes to the numerous distinct climatic zones. As expected, inland CBGs have more days that reach extremely high temperatures, as opposed to CBGs closer to the coast or San Francisco Bay (Figure S2). Due to this spatial variability, there is additional value in the location-based fixed effects of our panel regression.

Finally, the results of this study are specific only to 2020-2021, and there remain several questions about the long-term influence of the temporary COVID-driven mobility restrictions after SIP orders were lifted across California (Slavitt et al., 2022). These include any persistent changes to mobility as SIP policies relaxed, and whether extended restrictions led to changes in the services provided to different CBGs (including permanent closures of some services). It is possible that individuals now rely on new measures to alleviate heat stress at home—including investing in cooling technologies such as portable air conditioning units, window tinting, or improved insulation. Alternately, the lack of any pandemic-related mobility restrictions means the mobility-temperature relationship may begin to echo the patterns it once held prior to the March 2020 SIP orders. However, while the risks of contracting COVID-19 have been significantly reduced through vaccination, the pandemic was still on-going as of Fall 2022.



Individual sheltering and isolation guidelines continue to evolve, and we have yet to collect data on a period beyond 2021.

## 5 Conclusions

In addition to the primary health impacts of COVID-19, the pandemic has also had secondary impacts by affecting the ways in which individuals and communities are able to respond to other health risks, such as severe heat. In this study, we leveraged the variability in SIP policies and severity of COVID-19 transmission risk to explore how different income groups respond to severe heat under changing social and policy pressures.

We built upon prior studies of the relationship between heat and mobility using causal inference methods to explore how a unit change in temperature may change mobility. In particular, using panel regressions with fixed effects enabled us to control for unobserved variability between CBGs and counties (e.g., common behavior patterns, infrastructure) and changes that occur over time that are common across the CBGs or counties (e.g. federal or state-wide regulations). The results of this regression model with interaction variables allowed us to investigate how the median income of the observed CBG may influence the expected mobility during the hottest days of the year. We also leveraged a quantile regression model to investigate the relationship between MI and temperature, and explore various parts of the distribution independent from the rest of the dataset.

The patterns we uncovered add clarity to the previous understanding of the relationship between temperature and mobility (Böcker et al., 2016, Liu et al., 2014, Badr et al., 2020, Zhu et al., 2020) during a period when typical mobility patterns were already disrupted by COVID-19 policies. We show that during this pandemic period, wealthier CBGs have generally had lower mobility during periods of severe heat, compared with other income groups. Our results also suggest that there is a fundamental difference in the temperature-mobility relationship between the most mobile High and Low income CBGs, with High income CBGs further decreasing mobility in response to high temperatures, and lower income CBGs either increasing mobility (Figure 4) or decreasing at a slower rate (Figure 5). Thus, even in the presence of highly restrictive public health policies, high temperatures can lead to diverging mobility across income. Given the key role that mobility plays in public health interventions during periods of extreme heat, our results are relevant for heat mitigation efforts in highly populated regions, both in the current climate and in the future.

## Acknowledgments

We thank the Climatology Lab for access to the gridMET daily maximum temperature product, Safegraph and the Safegraph COVID-19 Data Consortium for access to daily mobility information, the Bay Area Air Quality Management District for aggregated daily air quality data, and the US Census Bureau and American Community Survey for providing median income and population data. Computational resources were provided by the Center for Computational Earth & Environmental Sciences and the Stanford Research Computing Center at Stanford University. Funding was provided by Stanford University.



## Open Research

The R scripts used to execute and report on the analyses in this paper can be found at [https://github.com/aminaly/heatwave\\_covid](https://github.com/aminaly/heatwave_covid), and is preserved at (DOI: [10.5281/zenodo.7434145](https://doi.org/10.5281/zenodo.7434145)).

## Availability Statement

SafeGraph's raw mobility data can be accessed through registration on their website, <https://www.safegraph.com/covid-19-data-consortium>. gridMET data are available online for download at <https://www.climatologylab.org/gridmet.html>. American Community Survey Data can be accessed on the US Census Bureau's website, <https://www.census.gov/programs-surveys/acs/data.html>.

## Conflict of Interest Statement

The authors have no conflicts of interest to declare.

## References

- Abatzoglou, J. T. (2013). Development of gridded surface meteorological data for ecological applications and modeling. *International Journal of Climatology*, 33(1), 121–131.  
<https://doi.org/10.1002/joc.3413>
- American Housing Survey (AHS). (2018). [Data set]. US Department of Housing and Urban Development. Retrieved from <https://catalog.data.gov/dataset/american-housing-survey-ahs>
- Aragón, Tomás J. "Travel Advisory." Travel Advisory, California Department of Public Health, <https://www.cdph.ca.gov/Programs/CID/DCDC/Pages/COVID-19/Travel-Advisory.aspx>
- Badr, H. S., Du, H., Marshall, M., Dong, E., Squire, M. M., & Gardner, L. M. (2020). Association between mobility patterns and COVID-19 transmission in the USA: a mathematical modelling study. *The Lancet Infectious Diseases*, 20(11), 1247–1254.  
[https://doi.org/10.1016/S1473-3099\(20\)30553-3](https://doi.org/10.1016/S1473-3099(20)30553-3)
- Banzhaf, H. S., Ma, L., & Timmins, C. (2019). Environmental Justice: Establishing Causal Relationships. *Annual Review of Resource Economics*, 11(1), 377–398.  
<https://doi.org/10.1146/annurev-resource-100518-094131>

- Bassil, K. L., Cole, D. C., Moineddin, R., Craig, A. M., Wendy Lou, W. Y., Schwartz, B., & Rea, E. (2009). Temporal and spatial variation of heat-related illness using 911 medical dispatch data. *Environmental Research*, 109(5), 600–606.  
<https://doi.org/10.1016/j.envres.2009.03.011>
- Basu, R., & Ostro, B. D. (2008). A Multicounty Analysis Identifying the Populations Vulnerable to Mortality Associated with High Ambient Temperature in California. *American Journal of Epidemiology*, 168(6), 632–637. <https://doi.org/10.1093/aje/kwn170>
- Batibeniz, F., Ashfaq, M., Diffenbaugh, N. S., Key, K., Evans, K. J., Turuncoglu, U. U., & Öno, B. (2020). Doubling of U.S. Population Exposure to Climate Extremes by 2050. *Earth's Future*, 8(4), e2019EF001421. <https://doi.org/10.1029/2019EF001421>
- Bay Area Air Quality Management District (BAAQMD). (2021). Spare the Air Every Day. Retrieved September 22, 2022, from <https://www.baaqmd.gov/alertstatus>
- Böcker, L., Dijst, M., & Faber, J. (2016). Weather, transport mode choices and emotional travel experiences. *Transportation Research Part A: Policy and Practice*, 94, 360–373.  
<https://doi.org/10.1016/j.tra.2016.09.021>
- Buchinsky, M. (1998). Recent Advances in Quantile Regression Models: A Practical Guideline for Empirical Research. *The Journal of Human Resources*, 33(1), 88–126.  
<https://doi.org/10.2307/146316>
- Burke, M., González, F., Baylis, P., Heft-Neal, S., Baysan, C., Basu, S., & Hsiang, S. (2018). Higher temperatures increase suicide rates in the United States and Mexico. *Nature Climate Change*, 8(8), 723–729. <https://doi.org/10.1038/s41558-018-0222-x>
- CDC. (2022, May 31). Extreme Heat. Retrieved November 28, 2022, from <https://www.cdc.gov/nceh/features/trackingheat/>

- Collins, M., Knutti, R., Arblaster, J., Dufresne, J.-L., Fichefet, T., Gao, X., et al. (n.d.). Long-term Climate Change: Projections, Commitments and Irreversibility, 108.
- Deschênes, O., Greenstone, M., & Guryan, J. (2009). Climate Change and Birth Weight. *American Economic Review*, 99(2), 211–217. <https://doi.org/10.1257/aer.99.2.211>
- Diffenbaugh, N. S., & Ashfaq, M. (2010). Intensification of hot extremes in the United States. *Geophysical Research Letters*, 37(15). <https://doi.org/10.1029/2010GL043888>
- Diffenbaugh, N. S., Field, C. B., Appel, E. A., Azevedo, I. L., Baldocchi, D. D., Burke, M., et al. (2020). The COVID-19 lockdowns: a window into the Earth System. *Nature Reviews Earth & Environment*, 1(9), 470–481. <https://doi.org/10.1038/s43017-020-0079-1>
- Diffenbaugh, N. S., Singh, D., & Mankin, J. S. (2018). Unprecedented climate events: Historical changes, aspirational targets, and national commitments. *Science Advances*, 4(2), eaao3354. <https://doi.org/10.1126/sciadv.aao3354>
- Downey, L. (1998). Environmental Injustice: Is Race or Income a Better Predictor? *Social Science Quarterly*, 79(4), 766–778. Retrieved from <https://www.jstor.org/stable/42863846>
- Duffy, P. B., Field, C. B., Diffenbaugh, N. S., Doney, S. C., Dutton, Z., Goodman, S., et al. (2019). Strengthened scientific support for the Endangerment Finding for atmospheric greenhouse gases. *Science*. <https://doi.org/10.1126/science.aat5982>
- Eisenman, D. P., Wilhalme, H., Tseng, C.-H., Chester, M., English, P., Pincetl, S., et al. (2016). Heat Death Associations with the built environment, social vulnerability and their interactions with rising temperature. *Health & Place*, 41, 89–99. <https://doi.org/10.1016/j.healthplace.2016.08.007>

- Ekstrom, J. A., & Moser, S. C. (2012). Climate Change Impacts, Vulnerabilities, and Adaptation in the San Francisco Bay Area: A Synthesis of PIER Program Reports and Other Relevant Research. Retrieved from <https://escholarship.org/uc/item/9qx629fh>
- Gronlund, C. J., & Berrocal, V. J. (2020). Modeling and comparing central and room air conditioning ownership and cold-season in-home thermal comfort using the American Housing Survey. *Journal of Exposure Science & Environmental Epidemiology*, 30(5), 814–823. <https://doi.org/10.1038/s41370-020-0220-8>
- Hansen, A., Bi, L., Saniotis, A., & Nitschke, M. (2013). Vulnerability to extreme heat and climate change: is ethnicity a factor? *Global Health Action*, 6(1), 21364. <https://doi.org/10.3402/gha.v6i0.21364>
- Head, J. R., Andrejko, K. L., Cheng, Q., Collender, P. A., Phillips, S., Boser, A., et al. (2020, August 7). The effect of school closures and reopening strategies on COVID-19 infection dynamics in the San Francisco Bay Area: a cross-sectional survey and modeling analysis. medRxiv. <https://doi.org/10.1101/2020.08.06.20169797>
- Hobbs, R. J., Richardson, D. M., & Davis, G. W. (1995). Mediterranean-Type Ecosystems: Opportunities and Constraints for Studying the Function of Biodiversity. In G. W. Davis & D. M. Richardson (Eds.), *Mediterranean-Type Ecosystems* (Vol. 109, pp. 1–42). Berlin, Heidelberg: Springer Berlin Heidelberg. [https://doi.org/10.1007/978-3-642-78881-9\\_1](https://doi.org/10.1007/978-3-642-78881-9_1)
- Hsiang, S. M., Burke, M., & Miguel, E. (2013). Quantifying the Influence of Climate on Human Conflict. *Science*, 341(6151), 1235367. <https://doi.org/10.1126/science.1235367>
- IPCC, 2021: Climate Change 2021: The Physical Science Basis. Contribution of Working Group I to the Sixth Assessment Report of the Intergovernmental Panel on Climate Change[Masson-Delmotte, V., P. Zhai, A. Pirani, S.L. Connors, C. Péan, S. Berger, N.

Caud, Y. Chen, L. Goldfarb, M.I. Gomis, M. Huang, K. Leitzell, E. Lonnoy, J.B.R. Matthews, T.K. Maycock, T. Waterfield, O. Yelekçi, R. Yu, and B. Zhou (eds.)). Cambridge University Press, Cambridge, United Kingdom and New York, NY, USA, In press, doi:10.1017/9781009157896.

Jung, Y. (2021, June 25). The Bay Area is getting hotter. Is air conditioning becoming standard for homes here? Retrieved November 28, 2022, from <https://www.sfchronicle.com/local/article/How-many-Bay-Area-homes-have-air-conditioning-16273057.php>

Liss, A., & Naumova, E. N. (2019). Heatwaves and hospitalizations due to hyperthermia in defined climate regions in the conterminous USA. *Environmental Monitoring and Assessment*, 191(2), 394. <https://doi.org/10.1007/s10661-019-7412-5>

Liu, C., Susilo, Y. O., & Karlström, A. (2014). Examining the impact of weather variability on non-commuters' daily activity–travel patterns in different regions of Sweden. *Journal of Transport Geography*, 39, 36–48. <https://doi.org/10.1016/j.jtrangeo.2014.06.019>

Luber, G., & McGeehin, M. (2008). Climate Change and Extreme Heat Events. *American Journal of Preventive Medicine*, 35(5), 429–435. <https://doi.org/10.1016/j.amepre.2008.08.021>

Newsom, G. (2020). Executive Order. No. N-33-20, 2020, p. 2., 2.

Obradovich, N., Migliorini, R., Mednick, S. C., & Fowler, J. H. (2017). Nighttime temperature and human sleep loss in a changing climate. *Science Advances*, 3(5), e1601555. <https://doi.org/10.1126/sciadv.1601555>

- O'Neill, M. S., Zanobetti, A., & Schwartz, J. (2003). Modifiers of the Temperature and Mortality Association in Seven US Cities. *American Journal of Epidemiology*, 157(12), 1074–1082.  
<https://doi.org/10.1093/aje/kwg096>
- O'Neill, M. S., Zanobetti, A., & Schwartz, J. D. (2005). Disparities by Race in Heat-Related Mortality in Four US Cities: The Role of Air Conditioning Prevalence. *Journal of Urban Health: Bulletin of the New York Academy of Medicine*, 82(2), 191–197.  
<https://doi.org/10.1093/jurban/jti043>
- Onozuka, D., & Hagihara, A. (2015). All-Cause and Cause-Specific Risk of Emergency Transport Attributable to Temperature. *Medicine*, 94(51), e2259.  
<https://doi.org/10.1097/MD.0000000000002259>
- Palecki, M. A., Changnon, S. A., & Kunkel, K. E. (2001). The Nature and Impacts of the July 1999 Heat Wave in the Midwestern United States: Learning from the Lessons of 1995. *Bulletin of the American Meteorological Society*, 82(7), 1353–1368.  
[https://doi.org/10.1175/1520-0477\(2001\)082<1353:TNAIOT>2.3.CO;2](https://doi.org/10.1175/1520-0477(2001)082<1353:TNAIOT>2.3.CO;2)
- Park, J., Pankratz, N. M. C., & Behrer, A. (2021, July 24). Temperature, Workplace Safety, and Labor Market Inequality. SSRN Scholarly Paper, Rochester, NY.  
<https://doi.org/10.2139/ssrn.3892588>
- Reid, C. E., O'Neill Marie S., Gronlund, C. J., Brines, S. J., Brown, D. G., Diez, -Roux Ana V., & Schwartz, J. (2009). Mapping Community Determinants of Heat Vulnerability. *Environmental Health Perspectives*, 117(11), 1730–1736.  
<https://doi.org/10.1289/ehp.0900683>
- Reidmiller, D. R., Avery, C. W., Easterling, D. R., Kunkel, K. E., Lewis, K. L. M., Maycock, T. K., & Stewart, B. C. (2018). *Impacts, Risks, and Adaptation in the United States: The*

*Fourth National Climate Assessment, Volume II.* U.S. Global Change Research Program.

<https://doi.org/10.7930/NCA4.2018>

SafeGraph. SafeGraph COVID-19 Data Consortium; 2020. Available from:

<https://www.safegraph.com/covid-19-data-consortium>.

San Francisco Department of Health (SFDH), Health Officer. Order of the Health Officer No.

C19-07 (Shelter in Place), 16 Mar. 2020.

<https://sfgsa.org/sites/default/files/Document/OrderC19-07ShelterinPlace.pdf>. Accessed 12

Jan. 2021.

Schwartz, J. D., Lee, M., Kinney, P. L., Yang, S., Mills, D., Sarofim, M. C., et al. (2015).

Projections of temperature-attributable premature deaths in 209 U.S. cities using a cluster-

based Poisson approach. *Environmental Health*, 14(1), 85. [https://doi.org/10.1186/s12940-](https://doi.org/10.1186/s12940-015-0071-2)

[015-0071-2](https://doi.org/10.1186/s12940-015-0071-2)

Shao, W., Xie, J., & Zhu, Y. (2021). Mediation by human mobility of the association between

temperature and COVID-19 transmission rate. *Environmental Research*, 194, 110608.

<https://doi.org/10.1016/j.envres.2020.110608>

Slavitt, A., Bibbins-Domingo, PhD, MD, MAS, K., & Wachter. (2022, February 17). Governor

Newsom Unveils SMARTER Plan Charting California's Path Forward on Nation-Leading

Pandemic Response. Retrieved September 26, 2022, from

[https://www.gov.ca.gov/2022/02/17/governor-newsom-unveils-smarter-plan-charting-](https://www.gov.ca.gov/2022/02/17/governor-newsom-unveils-smarter-plan-charting-californias-path-forward-on-nation-leading-pandemic-response/)

[californias-path-forward-on-nation-leading-pandemic-response/](https://www.gov.ca.gov/2022/02/17/governor-newsom-unveils-smarter-plan-charting-californias-path-forward-on-nation-leading-pandemic-response/)

Studdert, D. M., Hall, M. A., & Mello, M. M. (2020). Partitioning the Curve — Interstate Travel

Restrictions During the Covid-19 Pandemic. *New England Journal of Medicine*, 383(13),

e83. <https://doi.org/10.1056/NEJMp2024274>

- Tasian, G. E., Pulido, J. E., Gasparrini, A., Saigal, C. S., Horton, B. P., Landis, J. R., et al. (2014). Daily Mean Temperature and Clinical Kidney Stone Presentation in Five U.S. Metropolitan Areas: A Time-Series Analysis. *Environmental Health Perspectives*, 122(10), 1081–1087. <https://doi.org/10.1289/ehp.1307703>
- UNWTO. (2020). 100% of Global Destinations Now Have COVID-19 Travel Restrictions, UNWTO Reports | UNWTO. Retrieved January 10, 2022, from <https://www.unwto.org/news/covid-19-travel-restrictions>
- US Census Bureau. (2020). 2015-2019 American Community Survey Data. Retrieved January 12, 2022, from <https://www.census.gov/programs-surveys/acs/data.html>
- Vant-Hull, B., Ramamurthy, P., Havlik, B., Jusino, C., Corbin-Mark, C., Schuerman, M., et al. (2018). The Harlem Heat Project: A Unique Media–Community Collaboration to Study Indoor Heat Waves. *Bulletin of the American Meteorological Society*, 99(12), 2491–2506. <https://doi.org/10.1175/BAMS-D-16-0280.1>
- Vasireddy, D., Vanaparthi, R., Mohan, G., Malayala, S. V., & Atluri, P. (2021). Review of COVID-19 Variants and COVID-19 Vaccine Efficacy: What the Clinician Should Know? *Journal of Clinical Medicine Research*, 13(6), 317–325. <https://doi.org/10.14740/jocmr4518>
- Wainwright, S. H., Buchanan, S. D., Mainzer, M., Parrish, R. G., & Sinks, T. H. (1999). Cardiovascular Mortality — The Hidden Peril of Heat Waves. *Prehospital and Disaster Medicine*, 14(4), 18–27. <https://doi.org/10.1017/S1049023X00027679>
- WHO Director-General’s opening remarks at the media briefing on COVID-19 - 11 March 2020. (2020). Retrieved January 12, 2022, from <https://www.who.int/director-general/speeches/detail/who-director-general-s-opening-remarks-at-the-media-briefing-on-covid-19---11-march-2020>



Widerynski, S., Schramm, P., Conlon, K., Noe, R., Grossman, E., Hawkins, M., et al. (2017).

The Use of Cooling Centers to Prevent Heat-Related Illness: Summary of Evidence and

Strategies for Implementation (Climate and Health Technical Report Series). *Climate and*

*Health Program, Centers for Disease Control and Prevention.*

<https://stacks.cdc.gov/view/cdc/47657>

Wu, Y., Mooring, T. A., & Linz, M. (2021). Policy and weather influences on mobility during

the early US COVID-19 pandemic. *Proceedings of the National Academy of Sciences*,

118(22), e2018185118. <https://doi.org/10.1073/pnas.2018185118>

Zheng, G., Li, K., & Wang, Y. (2019). The Effects of High-Temperature Weather on Human

Sleep Quality and Appetite. *International Journal of Environmental Research and Public*

*Health*, 16(2), 270. <https://doi.org/10.3390/ijerph16020270>

Zhu, L., Liu, X., Huang, H., Avellán-Llaguno, R. D., Lazo, M. M. L., Gaggero, A., et al. (2020).

Meteorological impact on the COVID-19 pandemic: A study across eight severely affected

regions in South America. *Science of The Total Environment*, 744, 140881.

<https://doi.org/10.1016/j.scitotenv.2020.140881>

Zimmerman, F. J., & Anderson, N. W. (2019). Trends in Health Equity in the United States by

Race/Ethnicity, Sex, and Income, 1993-2017. *JAMA Network Open*, 2(6), e196386.

<https://doi.org/10.1001/jamanetworkopen.2019.6386>